Study on the magnetization reversal process in a magnetic nanowire and a magnetic dot observed by magnetic field sweeping magnetic force microscopy measurements (invited)

doi: 10.1063/1.2836681

Study on the magnetization reversal process in a magnetic nanowire and a magnetic dot observed by magnetic field sweeping magnetic force microscopy measurements (invited)

Yasushi Endo,[a] Hideki Fujimoto, Shinya Kumano, Yusuke Matsumura, Isao Sasaki, Yoshio Kawamura, and Masahiko Yamamoto
Department of Materials Science and Engineering, Graduate School of Engineering, Osaka University, 2-1 Yamadaoka, Suita 565-0871, Japan

Ryoichi Nakatani
Center for Atomic and Molecular Technologies, Graduate School of Engineering, Osaka University, 2-1 Yamadaoka, Suita 565-0871, Japan

(Presented on 6 November 2007; received 7 September 2007; accepted 4 November 2007; published online 13 February 2008)

We have studied the details of the magnetization reversal process in Ni–Fe nanowires and dots using magnetic field sweeping (MFS)-magnetic force microscopy (MFM). All the points within the nanowire and the dot show important changes in phase (changes in stray field) including a hysteresis loop, a decrease and an increase in phase, as the magnetic field is varied. From these results, it is demonstrated that domain wall motion dominates the magnetization reversal process of a 10-nm-thick Ni–Fe nanowire with widths between 100 and 1000 nm. It is also demonstrated that the nucleation, the movement, and the annihilation of the vortex core can be directly observed in the magnetization reversal process of a 40-nm-thick Ni–Fe circular dot with diameters between 200 and 800 nm. Furthermore, it is found that, in the magnetization reversal process of a 10-nm-thick Ni–Fe elliptical dot with several major axial distances between adjacent dots, the magnetization between the adjacent dots magnetostatically couples as the major axial distance decreases.
 [DOI: 10.1063/1.2836681]

I. INTRODUCTION

Magnetic properties of nanosized magnets with various shape and size have been studied intensively because nanosized magnets are candidates for practical applications, including nonvolatile magnetic random access memory (MRAM),[1–3] magnetic storage media,[4–6] and magnetic logic gate (MLG).[7–9] In particular, much attention has been focused on the studies of magnetization reversal process in a single nanosized magnet from both fundamental and applied points of views.[10–15] The understanding of the magnetostatic interaction between the adjacent nanosized magnets is also an important subject.[16–18] For these studies, an experimental technique to directly observe the details of magnetization reversal process in a single nanosized magnet is required.

Recently, we have proposed a new magnetization measurement method, magnetic field sweeping (MFS)-magnetic force microscopy (MFM),[19–21] which use a MFM tip as a detector while the magnetic field is swept. MFS-MFM has the following advantages: it can directly observe the precise magnetic state in a local point within a single nanosized magnet at room temperature, the shape of the specimens is not restricted, and the measuring time is less than 1 min. We have directly observed the movement and annihilation of the vortex core in an isolated Co–Fe dot using MFS-MFM.[19] We have also demonstrated that the domain wall is trapped in the constriction area for the Ni nanowire with the constriction[20] and that the dominant factor for magnetization reversal process in a Ni–Fe nanowire with width of 200 nm changes from domain wall motion to both domain wall motion and domain wall pinning as the thickness of the nanowire increases.[21] In this paper, we report, using MFS-MFM, the magnetization reversal process in a Ni–Fe nanowire with various widths, the magnetization reversal process in a Ni–Fe circular dot with different diameters, and study the effect on the magnetostatic interaction between the adjacent Ni–Fe elliptical dots.

II. EXPERIMENTAL PROCEDURES

Ni-20 at.%Fe(Ni–Fe) nanowires, circular dots, and elliptical dots were fabricated by electron-beam lithography and a lift-off technique onto thermally oxidized Si (100) substrates. Ni–Fe films were deposited by dc magnetron sputtering or electron-beam deposition. For the case of elliptical dots, a magnetic field of around 0.5 kOe was applied to the major axial direction of dots, which caused unidirectional anisotropy in the dots. For the nanowires, the thickness and the length were 10 and 2100 nm, respectively, while the widths varied between 100 and 1000 nm. For the circular dots, the thickness was fixed at 40 nm, and the diameter varied between 200 and 800 nm. For the elliptical dot array, the thickness, the length of the major axis, and the length of the minor axis were 10, 200, and 100 nm, respectively. The major axial distance between adjacent dots were 50 and

[a]Electronic mail: endo@mat.eng.osaka-u.ac.jp. Present address: Department of Electrical and Communication Engineering, Graduate School of Engineering, Tohoku University, Japan.

200 nm, respectively. The appearances of the nanowires and the dots were estimated by scanning electron microcopy (the images are not shown).

The magnetization process of nanowire arrays and dot arrays was investigated by magneto-optical Kerr effect (MOKE) magnetometry, while the magnetic state of a single nanowire and a single dot was observed using our proposed measurement method, namely, MFS-MFM.

In MFS-MFM, a MFM tip is used as a detector as the magnetic field is swept between +1.0 and −1.0 kOe, so that the magnetic state of a local point in a nanowire or a dot can be directly observed by measuring the phase (the stray field). The MFM tip used in this method is a Si cantilever coated with a 30-nm-thick CoPtCr film, which has a low magnetic moment and is initially magnetized in the perpendicular direction. This tip is fixed 10 nm above the surface at a point of interest within the nanowire or the dot, which is at a height much lower than that in a conventional MFM measurement. This condition guarantees the signal pick up process in the range of around 20 nm.[22] This measurement was carried out at room temperature in a vacuum near 10^{-1} Pa.

III. RESULTS AND DISCUSSION

A. Magnetization reversal process in a 10-nm-thick Ni–Fe nanowire with several widths

Figure 1 shows the curves of phase versus magnetic field (H) at various points in 10-nm-thick Ni–Fe nanowires with the widths of (a) 100 and (b) 400 nm, as measured by MFS-MFM. The magnetic field is applied in the longitudinal direction of the nanowire plane. Here, Figs. 1(a-1) and 1(b-1) show MFM images in a zero field of single Ni–Fe nanowires with the widths of 100 and 400 nm, which originate from a C state and a S state, respectively, as reported in Refs. 23 and 24. The specific place where each point was measured is denoted in Figs. 1(a-1) and 1(b-1), here, points 1–4 indicate measured points within the nanowire. For each nanowire, the points 1 and 4 [Figs. 1(a-2), 1(a-5), 1(b-2), and 1(b-5)] display a hysteresis loop of the phase, which is attributed to the magnetization reversal taking place at the edge of the nanowire. At points 2 and 3 [Figs. 1(a-3), 1(a-4), 1(b-3), and 1(b-4)], phase increases are observed at approximately ±0.20 and ±0.08 kOe, respectively. These behaviors are ascribed to the domain wall motion within the nanowire. The magnetic fields at which these phase increases are observed are similar to the switching field of each nanowire array measured by MOKE. Thus, these results demonstrate that the details of magnetization reversal process within a nanowire can be observed using MFS-MFM.

These results can be confirmed in 10-nm-thick Ni–Fe nanowires with different widths. The magnetic fields ($H_{\mathrm{MFS\text{-}MFM}}$) at which the phase increased were observed by MFS-MFM and are summarized in Fig. 2 as a function of the width of the nanowire. The switching field (H_{sw}) of the Ni–Fe nanowire array obtained by MOKE is also shown. As can be observed, $H_{\mathrm{MFS\text{-}MFM}}$ and H_{sw} show an important decrease as the width of the nanowire increases. This happens because the magnetostatic energy is reduced when the width of the nanowire increases.[25] The values of $H_{\mathrm{MFS\text{-}MFM}}$ and H_{sw}

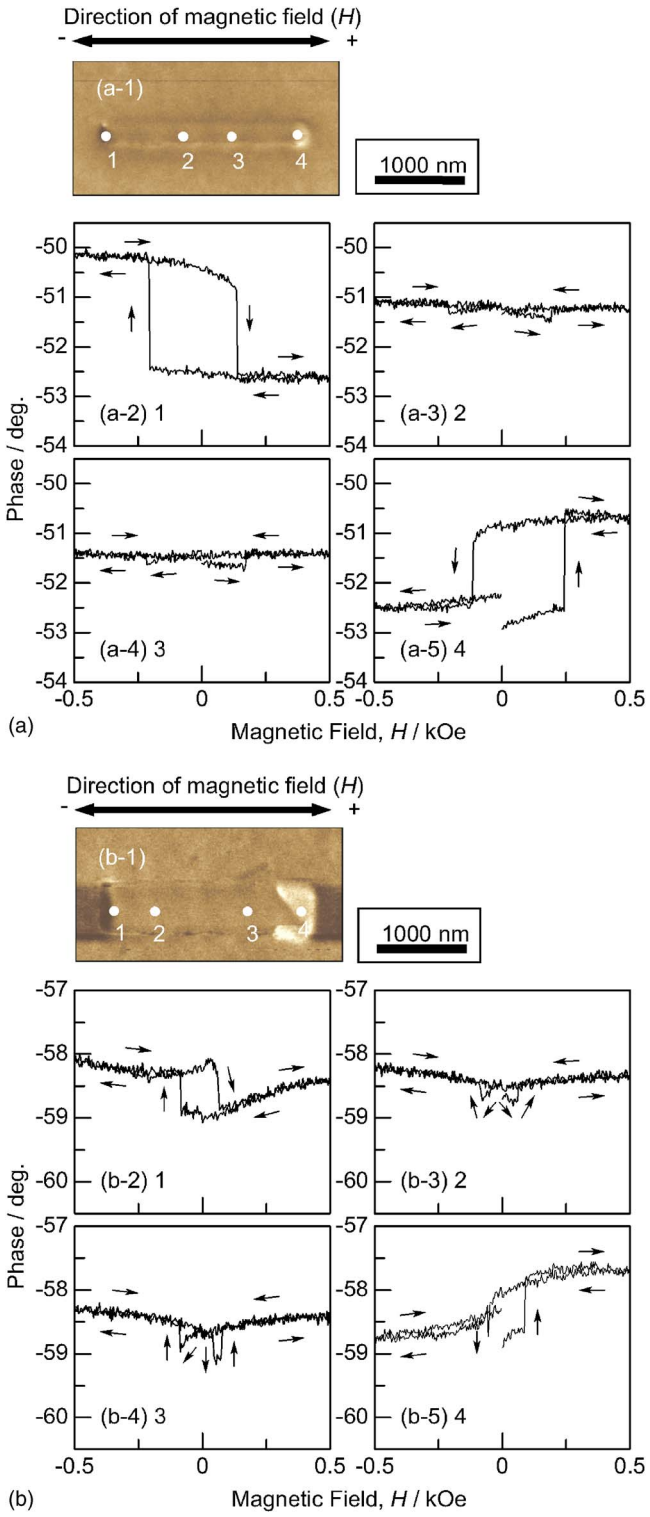

FIG. 1. (Color online) MFM images in a zero field of 10-nm-thick Ni–Fe nanowires with the widths of (a-1) 100 and (b-1) 400 nm. Points 1–4 indicate measured points within the nanowire. Curves of phase vs magnetic field (H) for various points in the Ni–Fe nanowires with the widths of (a-2)–(a-5) 100 and (b-2)–(b-5) 400 nm measured by MFS-MFM. The magnetic field is applied in the longitudinal direction of the nanowire plane.

are in good agreement, because H_{sw} is the average value of many nanowires and H_{sw} of each nanowire shows a wide distributed value in the MOKE loop. This result demonstrates that the switching field of a single nanowire can be measured by MFS-MFM. From these results and the origin

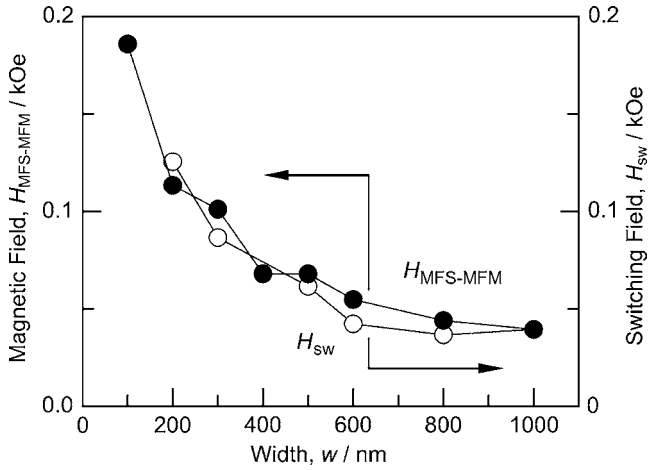

FIG. 2. Relationship between magnetic fields ($H_{MFS-MFM}$) at which the phase increases are observed by MFS-MFM and the switching field (H_{sw}) obtained by MOKE. The x axis indicates the widths of the nanowire. (●) and (○): $H_{MFS-MFM}$ and H_{sw}, respectively.

of the phase increases,[21] it can be said that the domain wall motion within the nanowire mainly dominates the magnetization reversal process of a 10-nm-thick Ni–Fe nanowire with various widths.

B. Magnetization reversal process in a 40-nm-thick Ni–Fe dot with several diameters

Figure 3 shows the curves of phase versus magnetic field (H) at various points in a 40-nm-thick Ni–Fe circular dot with the diameter of 500 nm, as measured by MFS-MFM. Figure 3(a) shows a MFM image in a zero field of a single Ni–Fe circular dot, which is derived from vortex core, as known from Ref. 26. The specific position of each point measured is denoted in Fig. 3(a). In this figure, the points 1 and 2 are parallel to the magnetic field and points 3–6 are perpendicular to the magnetic field. At points 1 and 2 [Figs. 3(b) and 3(c)], which are parallel to the magnetic field, the phase curves versus magnetic field are similar to the well-known MOKE loops showing the vortex formation.[27] On the other hand, all the points within the dot, which are perpendicular to the magnetic field, show important phase changes as the magnetic field is varied. At points 3 and 4 [Figs. 3(d) and 3(e)], a sharp valley of the measured phase is observed between −0.25 and −0.15 or 0.25 and 0.15 kOe as the magnetic field is changed from negative to positive or vice versa. These valleys are attributed to the nucleation of the vortex core at the dot edge. The ranges of magnetic field in which these valleys are observed are similar to that of the nucleation field of the circular dot array measured by MOKE. At point 5 [Fig. 3(f)], a weak dip is observed around zero field as the magnetic field is swept. It is originated from the movement of the vortex core. At point 6 [Fig. 3(g)], a mount of the phase is observed between 0.20 and 0.40 kOe as the magnetic field is changed from negative to positive, while a valley of the phase is observed between −0.20 and −0.40 kOe as the magnetic field is changed from positive to negative. These phase changes are due to the annihilation of the vortex core at the dot edge. The difference in sign due to the phase change might be related to the magnetization direction

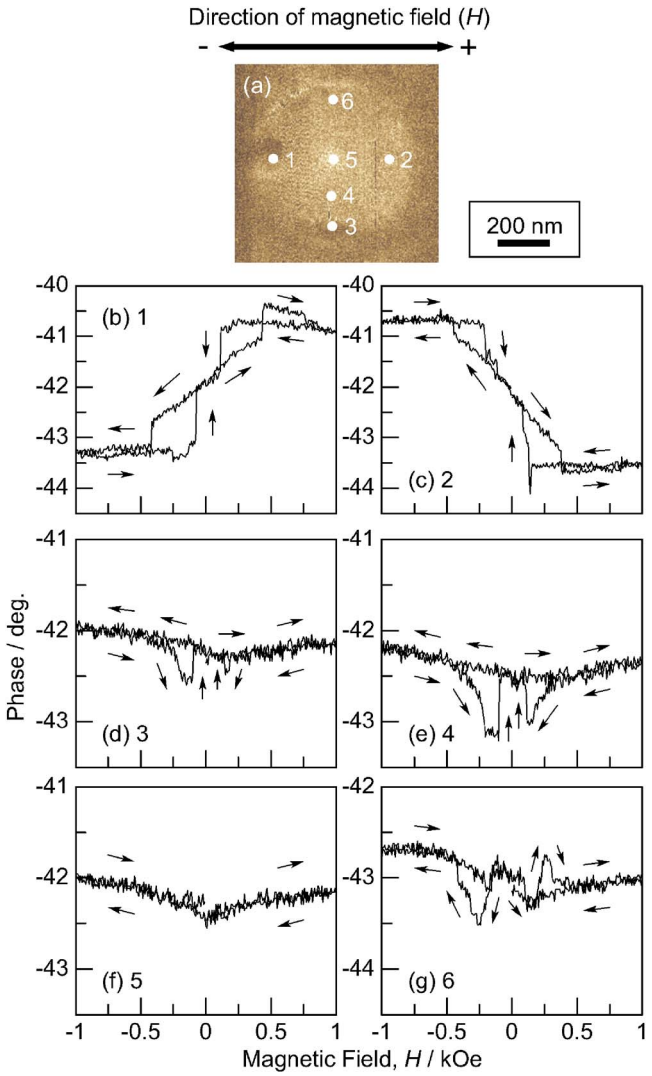

FIG. 3. (Color online) (a) MFM images in a zero field of 40-nm-thick Ni–Fe circular dot with the diameter of 500 nm. Points 1–6 indicate measured points within the circular dot. [(b)–(g)] Curves of phase vs magnetic field (H) for various points measured by MFS-MFM. The magnetic field is applied in the dot plane.

around the vortex core. Moreover, the ranges of magnetic field in which these phase changes occur are similar to those of the annihilation field for the circular dot array measured by MOKE.

These results can also be confirmed in 40-nm-thick Ni–Fe circular dots with diameters between 200 and 800 nm. As mentioned above, not only the movement and the annihilation of the vortex core but also the nucleation of the vortex core in a 40-nm-thick Ni–Fe circular dot with various diameters can be directly observed by MFS-MFM. The nucleation field (H_n) and the annihilation field (H_{an}) measured by MFS-MFM are summarized in Fig. 4 as a function of the diameter for a single circular dot. In this figure, H_n and H_{an} of the Ni–Fe circular array obtained by MOKE are also shown. For each of the above mention measurement, H_n and H_{an} decrease as the diameter of the circular dot increases. The reason for these is that both the anisotropy and exchange energies are reduced increasing the dot diameter.[25] H_n and H_{an} values measured by MFS-MFM are different from those ob-

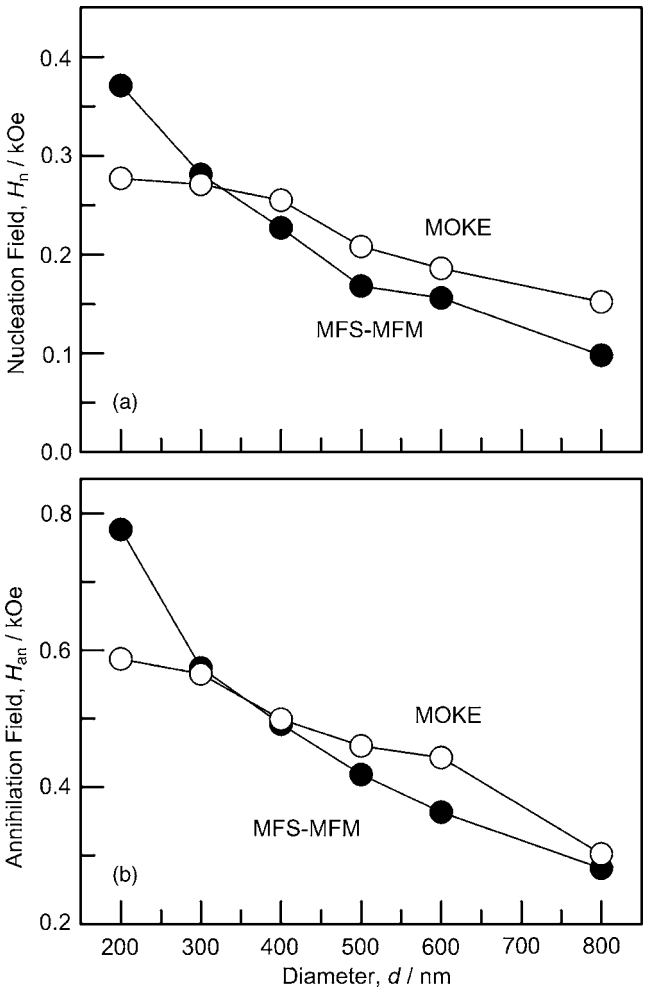

FIG. 4. Dependence of the nucleation field (H_n) and the annihilation field (H_{an}) in 40-nm-thick Ni–Fe circular dots on the diameter. (●) and (○): these fields measured by MFS-MFM and MOKE, respectively.

tained by MOKE, because these fields obtained by MOKE are widely distributed in the loop owing to the difference of the shape and the size in each circular dot. These results demonstrate that both the nucleation and annihilation fields at a single circular dot can be measured by MFS-MFM. Consequently, it is found that the vortex core within the dot plays an important role in the magnetization reversal process of a 40-nm-thick Ni–Fe circular dot with diameters between 200 and 800 nm.

C. Effect on the magnetostatic interaction between adjacent Ni–Fe elliptical dots

As mentioned above, the details of the magnetization reversal process within a nanowire and a circular dot can be observed using MFS-MFM. In this section, we observe the magnetization reversal process in Ni–Fe elliptical dots using MOKE and MFS-MFM, and report the effect on the magnetostatic interaction between the adjacent Ni–Fe elliptical dots with different major axial distances between the adjacent dots.

Figure 5 shows MOKE loops in 10-nm-thick Ni–Fe elliptical dot arrays with different distances between the adjacent dots. The magnetic field is applied in the major axial

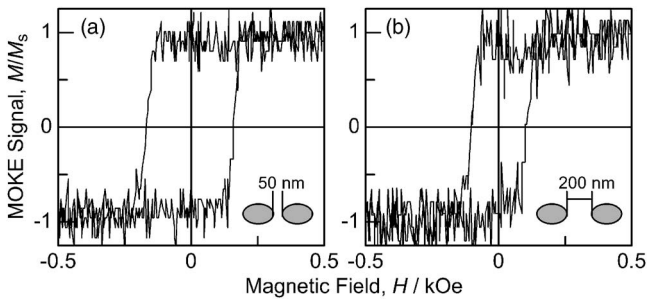

FIG. 5. MOKE loops of 10-nm-thick Ni–Fe elliptical dot arrays with different major axial distances between the adjacent dots of (a) 50 and (b) 200 nm. The magnetic field is applied in the major axial direction of the dot.

direction of the dot. The MOKE loop changes from a square shape [Fig. 5(a)] to a nearly square shape [Fig. 5(b)] as the distance between the adjacent dots increases. The coercivity also decreases as the major axial distance between the adjacent dots increases. These results might be caused by the reduction of the magnetostatic interaction that occurs when the distance between the adjacent dots increases.

In order to clarify the origin of the change in the magnetic properties of the Ni–Fe elliptical dot arrays with different distances between the adjacent dots, we investigated the details of the magnetization reversal process in these dots using MFS-MFM. Figure 6 shows the curves of phase versus magnetic field (H) at different points in a 10-nm-thick Ni–Fe circular dot with the major axial distance between the adjacent dots of (a) 50 and (b) 200 nm measured by MFS-MFM. Figures 6(a–1) and 6(b–1) show atomic force microscopy (AFM) image of a single Ni–Fe circular dot, and the position of each measurement is denoted in Figs. 6(a–1) and 6(b–1). Points 1–3 indicate the measured points within the dot. For the dot with the major axial distance between the adjacent dots of 50 nm, points 1 and 3 [Figs. 6(a–2) and 6(a–4)] each display a hysteresis loop of the phase. At point 2 [Figs. 6(a–3)], phase increases are observed at approximately −0.20 and +0.15 kOe. The magnetic fields at which these phase increases are observed are similar to the switching field of the dot array measured by MOKE [Fig. 5(a)]. These results almost coincide with those of a 10-nm-thick Ni–Fe nanowire, as can be seen in Fig. 1 (Sec. III A). The above observations of the dot mean that the magnetic state of the dot changes from a single domain (SD) state to an opposite SD state as the magnetic field is varied, and that the magnetization coherently rotates. On the other hand, for the dot with the distance between the adjacent dots of 200 nm, points 1 and 3 [Figs. 6(a–2) and 6(a–4)] each display a stepped hysteresis loop of the phase. At point 2 [Figs. 6(a–3)], phase decreases are observed at approximately a zero field. These results reveal that the magnetic state of the dot changes from a SD state to a closure domain state, and further to an opposite SD state as the magnetic field is varied, and that the magnetization randomly rotates. Thus, the magnetization reversal process apparently differs according to the distance between the adjacent dots. This difference is due to the fact that the magnetostatic interaction is reduced while increasing the distance between the adjacent dots. Therefore, it is evident that the magnetostatic interaction strongly influences the magnetiza-

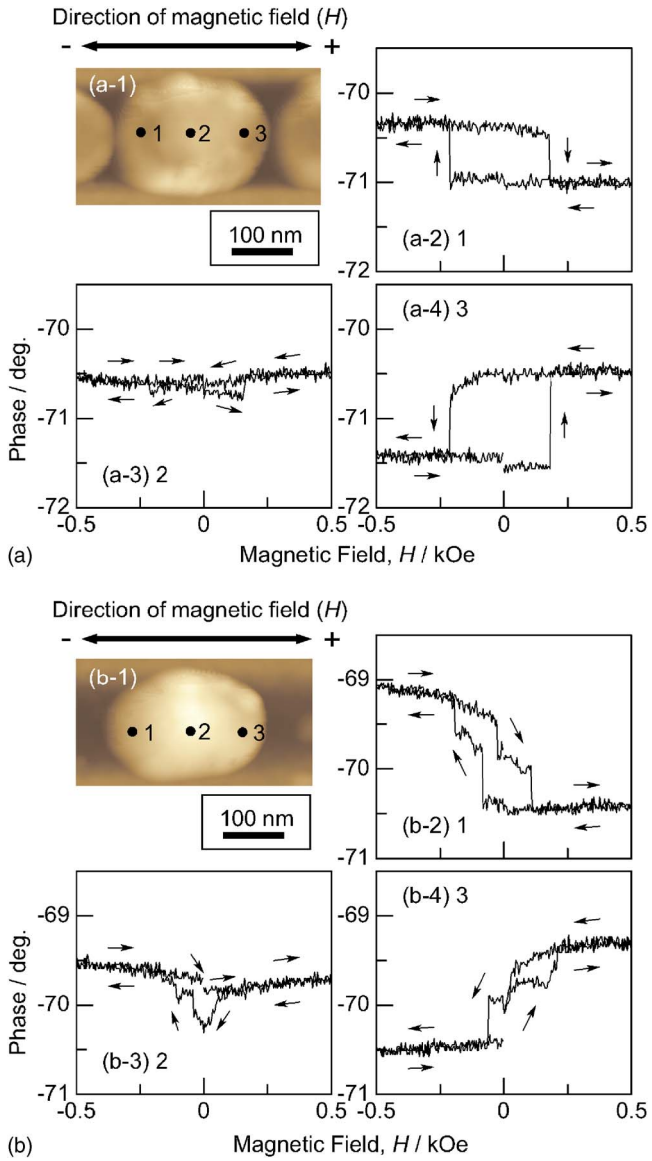

FIG. 6. (Color online) AFM images of 10-nm-thick Ni–Fe elliptical dots with the major axial distance between the adjacent dots of (a–1) 50 and (b–1) 200 nm. Points 1–3 indicate measured points within the dot. Curves of phase vs magnetic field (H) for various points in the Ni–Fe elliptical dots with the distances of (a–2)–(a–4) 50 and (b–2)–(b–4) 200 nm measured by MFS-MFM. The magnetic field is applied in the major axial direction of the dot.

tion reversal process in a 10-nm-thick Ni–Fe elliptical dot as the distance between the adjacent dots decreases.

IV. CONCLUSIONS

The details of the magnetization reversal process of Ni–Fe nanowires and Ni–Fe dots have been successfully observed using magnetic field sweeping magnetic force microscopy. For each 10-nm-thick Ni–Fe nanowire with the width between 100 and 1000 nm, a hysteresis loop of the phase (stray field) is observed in both edges, while the center displays jumps of the phase. These results demonstrate that domain wall motion plays an important role in the magnetization reversal process of single Ni–Fe nanowires. For each 40-nm-thick Ni–Fe circular dot with diameters between 200 and 800 nm, all the points within the dot, which are perpendicular to the magnetic field, show important phase changes as the magnetic field is varied. These results are attributed to the nucleation, the movement, and the annihilation of the vortex core. Furthermore, for a 10-nm-thick Ni–Fe elliptical dot with different major axial distances between the adjacent dots, the phase curve versus magnetic field apparently differs according to the distance between the adjacent dots. These results reveal that the magnetization between the adjacent dots magnetostatically couples as the distance decreases.

ACKNOWLEDGMENTS

This work was partly supported by a Grant-in-Aid for Scientific Research (S), Exploratory Research and Encouragement of Young Scientists (B) from the Japanese Ministry of Education, Culture, Sports, Science and Technology. This study was supported by Priority Assistance for the Formation of Worldwide Renowned Centers of Research—The Global COE Program (Project: Center of Excellence for Advanced Structural and Functional Materials Design) from the Ministry of Education, Culture, Sports, Science and Technology (MEXT), Japan.

[1] S. S. P. Parkin, K. P. Roche, M. G. Samant, P. M. Rice, R. B. Beyers, R. E. Scheuerlein, E. J. O'Sullivan, S. L. Brown, J. Bucchigano, D. W. Abraham, Yu Lu, M. Rooks, P. L. Trouilloud, R. A. Wanner, and W. J. Gallagher, J. Appl. Phys. **85**, 5828 (1999).
[2] J. G. Zhu, Y. Zheng, and G. A. Prinz, J. Appl. Phys. **87**, 6668 (2000).
[3] R. Nakatani, T. Yoshida, Y. Endo, Y. Kawamura, M. Yamamoto, T. Takenaga, S. Aya, T. Kuroiwa, S. Beysen, and H. Kobayashi, J. Magn. Magn. Mater. **286**, 31 (2005).
[4] S. Y. Chou, P. R. Krauss, and L. Kong, J. Appl. Phys. **79**, 6101 (1996).
[5] C. Hagioya, K. Koike, Y. Hirayama, J. Yamamoto, M. Ishibashi, O. Kitakami, and Y. Shimada, Appl. Phys. Lett. **75**, 3159 (1996).
[6] J. Moritz, L. Buda, B. Dieny, J. P. Nozières, R. J. M. van de Veerdonk, T. M. Crawford, and D. Weller, Appl. Phys. Lett. **84**, 1519 (2004).
[7] S. A. Haque, M. Yamamoto, R. Nakatani, and Y. Endo, J. Magn. Magn. Mater. **282**, 380 (2004).
[8] A. Imre, G. Csabe, L. Ji, A. Orlov, G. H. Bernstein, and W. Porod, Science **311**, 205 (2006).
[9] R. E. Herbert, S. A. Haque, and T. Hesjedal, J. Appl. Phys. **101**, 09F503 (2007).
[10] W. Wernsdorfer, B. Doudin, D. Mailly, K. Hasselbach, A. Benoit, J. Meier, J.-Ph. Ansermet, and B. Barbara, Phys. Rev. Lett. **77**, 1873 (1996).
[11] F. G. Monzon, D. S. Patterson, and M. L. Roukes, J. Magn. Magn. Mater. **195**, 19 (1999).
[12] J. Bekaert, D. Buntinx, C. Van Haesendonck, V. V. Moshchalkov, J. De Boeck, G. Borghs, and V. Metlushko, Appl. Phys. Lett. **81**, 3413 (2002).
[13] N. Kikuchi, S. Okamoto, O. Kitakami, Y. Shimada, and K. Fukamichi, Appl. Phys. Lett. **82**, 4313 (2003).
[14] T. A. Moore, T. J. Hayward, D. H. Y. Tse, J. A. C. Bland, F. J. Castaño, and C. A. Ross, J. Appl. Phys. **97**, 063910 (2005).
[15] M. V. Rastei, R. Meckenstock, and J. P. Bucher, Appl. Phys. Lett. **87**, 222505 (2005).
[16] M. Natali, I. L. Prejbeanu, A. Lebib, L. D. Buda, K. Ounadjela, and Y. Chen, Phys. Rev. Lett. **88**, 157203 (2002).
[17] V. Novosad, M. Grimsditch, J. Darrouzet, J. Pearson, S. D. Bader, V. Metlushko, K. Guslienko, Y. Otani, H. Shima, and K. Fukamichi, Appl. Phys. Lett. **82**, 3716 (2003).
[18] D. W. Abraham and Y. Lu, J. Appl. Phys. **98**, 023902 (2005).
[19] Y. Endo, H. Fujimoto, Y. Kawamura, R. Nakatani, and M. Yamamoto, J. Magn. Magn. Mater. **310**, 2436 (2007).
[20] J. Sato, Y. Endo, Y. Shiratsuchi, Y. Kawamura, R. Nakatani, M. Yamamoto, Y. Murakami, and A. Takahashi, Jpn. J. Appl. Phys., Part 1 **46**, 4117 (2007).
[21] Y. Endo, Y. Matsumura, H. Fujimoto, R. Nakatani, and M. Yamamoto, Jpn. J. Appl. Phys., Part 2 **46**, L898 (2007).
[22] T. Yamaoka, K. Watanabe, Y. Shirakawabe, and K. Chinone, J. Magn. Soc. Jpn. **27**, 429 (2003).
[23] W. Rave and A. Hubert, IEEE Trans. Magn. **36**, 3886 (2000).

[24]X. Liu, J. N. Chapman, S. McVitie, and C. D. W. Wilkinson, Appl. Phys. Lett. **84**, 4406 (2004).
[25]*Hysteresis in Magnetism For Physists, Materials Sicentists, and Engineers*, edited by G. Bertotti (Academic, San Diego, 1998).
[26]T. Shinjo, T. Okuno, R. Hassdorf, K. Shigeto, and T. Ono, Science **289**, 930 (2000).
[27]R. P. Cowburn, D. K. Koltsov, A. O. Adeyeye, M. E. Welland, and D. M. Tricker, Phys. Rev. Lett. **83**, 1042 (1999).